Lattice Dynamics of Potassium Chloride*

J. R. D. COPLEY,† R. W. MACPHERSON,† AND T. TIMUSK
Department of Physics and Institute for Materials Research, McMaster University, Hamilton, Ontario, Canada
(Received 6 January 1969)

Phonon dispersion curves along the [00ζ], [0ζ1], [0ζζ], and [ζζζ] directions in KCl at 115°K have been measured by inelastic scattering of slow neutrons using the McMaster University triple-axis spectrometer at Chalk River. Various versions of the shell model have been fitted to the measurements. They are also compared with Kucher's predictions and with the results of Schröder's breathing-shell model. Several quantities are calculated using the best-fit shell model. The main features of the frequency distribution function do not, in general, occur at the frequencies of the symmetry points X and L. The most prominent peak in the frequency distribution is at 155 cm^{-1}. It agrees with the strongest peak in the Raman spectrum of KCl. The Debye temperature, the Debye-Waller factor, and the inelastic structure factor are also calculated.

I. INTRODUCTION

THE lattice vibrations of most of the common alkali-halide crystals have been investigated by slow neutron spectroscopy and by diffuse x-ray scattering. The most complete measurements to date have been made on LiF,[1] NaF,[2] NaCl,[3] NaI,[4] KBr,[5] and KI [6] by neutron spectroscopy and on NaF [7] and NaCl [8] by x-ray scattering. Potassium chloride is perhaps the most obvious crystal still missing from this list and although some diffuse x-ray measurements exist for KCl [9,10] there are several reasons why a more complete investigation of the lattice vibrations should be undertaken.

Work on the optical properties[11] of both pure and defect-containing crystals has demonstrated that for a full understanding of the influence of the lattice vibrations, detailed dynamic models based on neutron spectroscopy are essential. KCl is a good material for optical studies of all kinds because it can be prepared more easily in highly pure form than some of the other alkali halides. For this reason a large amount of experimental work has been done on this substance. KCl has long been a favorite in color-center research.

From a lattice dynamics point of view, KCl is also of special interest. A number of good measurements of its macroscopic properties have been made, and it has been possible to calculate dispersion curves from these data using several theoretical models. Noteworthy among these calculations are those of Tolpygo and co-workers,[12,13] of Hardy,[14] and more recently of Schröder.[15] It is of interest to compare these predictions of the phonon frequencies with actual measurements. A survey of models of this type may help us towards a better understanding of lattice dynamics from a microscopic point of view.

In Sec. II we review briefly the experimental techniques. The measured frequencies at various points along symmetry directions are given in Sec. III. The predictions of models based on macroscopic parameters are compared with experiment in Sec. IV. The shell model used by Woods *et al.*[4] and by Cowley *et al.*[16] is introduced and least-squares fits of this model to the measurements are given. In Sec. V the results of several calculations using the best least-squares-fit model are presented and compared with results of other experiments.

II. MEASUREMENTS

The phonon dispersion curves of KCl were measured by slow neutron inelastic scattering using the McMaster University triple-axis spectrometer at Chalk River.[17] This instrument uses twin monochromating crystals which produce a beam of neutrons of energy E_0 and wave vector $\mathbf{k}_0$ normal to the reactor face. Neutrons of energy E' and wave vector $\mathbf{k}'$, scattered from the speci-

* Work supported in part by the National Research Council of Canada and in part by the Alfred P. Sloan Foundation.
† National Research Council of Canada Studentship holder.
[1] G. Dolling, H. G. Smith, R. M. Nicklow, P. R. Vijayaraghavan, and M. K. Wilkinson, Phys. Rev. **168**, 970 (1968).
[2] W. J. L. Buyers, Phys. Rev. **153**, 923 (1967).
[3] L. Almqvist, G. Raunio, and R. Stedman, in *Neutron Inelastic Scattering* (International Atomic Energy Agency, Vienna, 1968), Vol. I, p. 295; G. Raunio, L. Almqvist, and R. Stedman, Phys. Rev. **178**, 1496 (1969).
[4] A. D. B. Woods, W. Cochran, and B. N. Brockhouse, Phys. Rev. **119**, 980 (1960).
[5] A. D. B. Woods, B. N. Brockhouse, R. A. Cowley, and W. Cochran, Phys. Rev. **131**, 1025 (1963).
[6] G. Dolling, R. A. Cowley, C. Schittenhelm, and I. M. Thorson, Phys. Rev. **147**, 577 (1966).
[7] J. D. Pirie and T. Smith, J. Phys. **C1**, 648 (1968).
[8] W. J. L. Buyers and T. Smith, Phys. Rev. **150**, 758 (1966).
[9] N. Boccara, Compt. Rend. **250**, 1025 (1960).
[10] V. I. Iveronova, Parangtopo, and A. P. Zvyagina, Fiz. Tverd. Tela **9**, 1609 (1967) [English transl.: Soviet Physics—Solid State **9**, 1265 (1967)].
[11] For recent reviews on localized vibrations see A. A. Maradudin, in *Solid State Physics*, edited by F. Seitz and D. Turnbull (Academic Press Inc., New York, 1966), Vols. 18 and 19; see also M. V. Klein, in *Physics of Color Centres*, edited by W. B. Fowler (Academic Press Inc., New York, 1968).
[12] K. B. Tolpygo and I. G. Zaslavskaya, Trudy Inst. Fiz. Acad. Nauk Ukr., SSR, No. 4, 71 (1953) [English transl.: United Kingdom Atomic Energy Authority, Harwell Report AERE-transl. 972 (1963) (unpublished)].
[13] T. I. Kucher, Zh. Eksperim. i Teor. Fiz. **32**, 498 (1957) [English transl.: Soviet Phys.—JETP **5**, 418 (1957)].
[14] J. R. Hardy, Phil. Mag. **7**, 315 (1962).
[15] U. Schröder, Solid State Commun. **4**, 347 (1966).
[16] R. A. Cowley, W. Cochran, B. N. Brockhouse, and A. D. B. Woods, Phys. Rev. **131**, 1030 (1963).
[17] B. N. Brockhouse, G. A. de Wit, E. D. Hallman, and J. M. Rowe, in *Neutron Inelastic Scattering* (International Atomic Energy Agency, Vienna, 1968), Vol. II, p. 259.

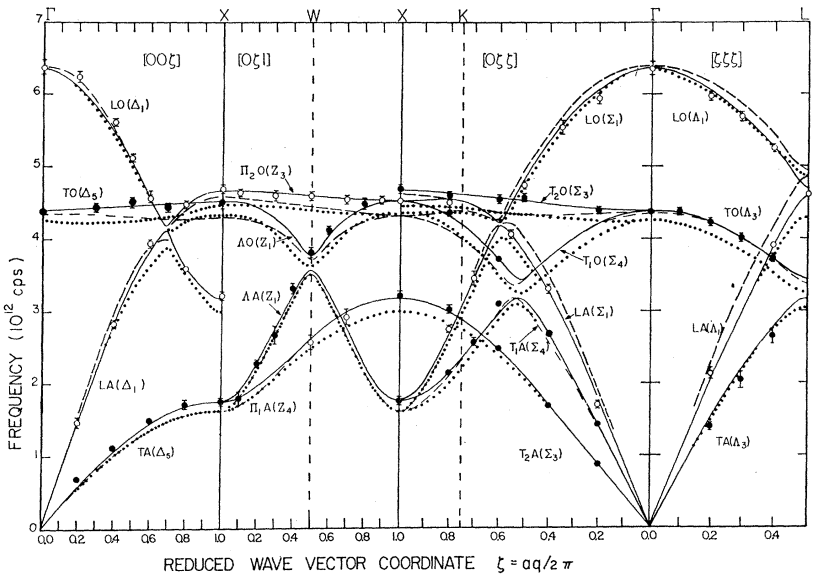

FIG. 1. Dispersion curves along major symmetry directions in KCl at 115°K. The open and filled circles denote the measured phonons. The solid line shows the model-VI fit. The dashed lines represent the breathing-shell-model calculation using parameters deduced from macroscopic data (model III). The dotted lines are the predictions of Kucher. The notation is explained in the text. The $\Pi_2A(Z_3)$ and $\Pi_1O(Z_4)$ branches are omitted for clarity.

men and selected by the analyzing crystal, are counted using a He^3 neutron detector.

In a one-phonon coherent scattering process, energy and wave vector are conserved[18]:

$$E_0-E'=(\hbar^2/2m_N)(k_0^2-k'^2)=\pm h\nu, \quad (1)$$

$$\mathbf{k}_0-\mathbf{k}'=\mathbf{Q}=2\pi\boldsymbol{\tau}+\mathbf{q}, \quad (2)$$

where m_N is the mass of the neutron, $\mathbf{Q}$ is the wave-vector transfer, and $\boldsymbol{\tau}$ is a reciprocal-lattice vector. The upper (lower) sign in Eq. (1) refers to phonon creation (annihilation). In this approximation the frequency ν and wave vector $\mathbf{q}$ of the phonon obey the dispersion relation $\nu=\nu_j(\mathbf{q})$, where j is the branch index; for a crystal having n atoms per (primitive) unit cell, the dispersion relation has $3n$ branches. The constant-$\mathbf{Q}$ method[19] was used throughout this experiment. Fixed incident neutron wavelengths, $2\pi/k_0$, between 1.425 and 1.335 Å, were employed, corresponding to frequencies between 9.75×10^{12} cps (325 cm^{-1}) and 11.09×10^{12} cps (370 cm^{-1}), and only neutron energy-loss (i.e., phonon creation) processes were examined.

The specimen, obtained from the Harshaw Chemical Co., was a cleaved single crystal of potassium chloride, $2\frac{1}{2}\times2\frac{1}{2}\times\frac{3}{4}$ in. with faces parallel to {200} planes. Measurements were made in the (100) and (1$\bar{1}$0) scattering planes. Where possible, measurements were made so that the path of the beam through the crystal was not too long, owing to the appreciable (34 b) absorption cross section[20] of chlorine.

The crystal was mounted in a metal cryostat and cooled from above to 115±5°K.

III. RESULTS

The measured phonons are shown in Fig. 1 and listed in Table I. The branches are labelled according to their polarization relative to $\mathbf{q}$. The [0ζζ] T_1 and T_2 branches are polarized parallel to [01$\bar{1}$] and [100], respectively, and the [0ζ1] Λ, Π_1, and Π_2 branches have polarization vectors parallel to [010], [100], and [001], respectively. The [0ζ1] branches are symmetrical about the point W, and, to avoid confusion, two of the Π branches have been omitted from the figure. The components of $\mathbf{q}$ are given in units of $2\pi/a$.

For any wave vector $\mathbf{q}$, along these symmetry directions, there are two branches of each polarization. The lower branch is labelled A (acoustic) and the upper branch is labelled O (optic).

The dispersion curves in Fig. 1 are also labelled according to the irreducible representations of the wave vector, using the notation of Bouckaert *et al.*[21]

From a consideration of the inelastic structure factor (see Sec. V) each group has been unambiguously assigned to a branch of the dispersion curves. Where two branches of the same polarization come close to each other, no difficulty was encountered in branch assignment, since the structure factors for A and O branches differ markedly at these points. The point $(\frac{1}{2},\frac{1}{2},\frac{1}{2})$ is not as well determined as some of the other symmetry points, since it was difficult to obtain good neutron groups at this point.

The errors assigned to the measured frequencies are normally $\pm0.1\Gamma$, where Γ is the width (full width at

[18] G. Placzek and L. Van Hove, Phys. Rev. **93**, 1207 (1954).

[19] B. N. Brockhouse, in *Inelastic Scattering of Neutrons in Solids and Liquids* (International Atomic Energy Agency, Vienna, 1961), p. 113.

[20] *Neutron Cross Sections, Brookhaven National Laboratory Report No. 325* compiled by D. J. Hughes and R. B. Schwartz (U. S. Government Printing Office, Washington, D. C., 1958), 2nd ed.

[21] L. P. Bouckaert, R. Smoluchowski, and E. Wigner, Phys. Rev. **50**, 58 (1936).

TABLE I. Normal-mode frequencies of KCl measured at 115°K. The branch index j is shown. The frequencies are in units of 10^{12} cps.

$\zeta=aq/2\pi$	ν (Acoustic)	j	ν (Optic)	j
[00ζ] T				
0.0			4.39 ±0.03	4,5
0.2	0.69 ±0.03	1,2		
0.3			4.44_5±0.05	4,5
0.4	1.12_5±0.03	1,2		
0.5			4.53 ±0.1	4,5
0.6	1.50 ±0.03	1,2		
0.7			4.45 ±0.05	5,6
0.8	1.72 ±0.05	1,2		
1.0	1.76 ±0.05	1,2	4.53 ±0.05	4,5
[00ζ] L				
0.0			6.39 ±0.1	6
0.2	1.47 ±0.08	3	6.25 ±0.08	6
0.4	2.83 ±0.08	3	5.55 ±0.04	6
0.5			5.13 ±0.03	6
0.6	3.95 ±0.06	3	4.58 ±0.05	6
0.8	3.59 ±0.04	3	4.49 ±0.05	6
1.0	3.23 ±0.05	3	4.70 ±0.05	6
[0ζζ] T_1				
0.2	1.43 ±0.02	2		
0.4	2.69 ±0.02	2		
0.6	3.10 ±0.1	2	3.73 ±0.03	3
0.7	2.57 ±0.04	1		
0.8	2.16 ±0.03	1	4.38 ±0.06	4
[0ζζ] T2				
0.2	0.89 ±0.03	1	4.41 ±0.05	5
0.4	1.67 ±0.02_5	1		
0.5			4.57 ±0.06	5
0.6	2.47_5±0.02_5	1	4.56 ±0.06	6
0.8	3.02_5±0.04_5	3	4.60_5±0.04	6
[0ζζ] L				
0.2	1.71 ±0.06	3	5.96 ±0.08	6
0.35			5.56 ±0.1	6
0.4	3.31 ±0.06	3		
0.5			4.75 ±0.06	6
0.55	4.08 ±0.06	4		
0.7	3.46 ±0.05	3		
0.8	2.75 ±0.06	2	4.51 ±0.05	5
[ζζζ] T				
0.1			4.37 ±0.04	4,5
0.2	1.41 ±0.05	1,2	4.23 ±0.06	4,5
0.3	2.04 ±0.15	1,2	4.02 ±0.04	4,5
0.4	2.64 ±0.13	1,2	3.72 ±0.04	3,4
[ζζζ] L				
0.2	2.12 ±0.04	3	5.97 ±0.04	6
0.3			5.70 ±0.07	6
0.4	3.91 ±0.03	5	5.25 ±0.05	6
0.5	4.60 ±0.02	5		
[0ζ1] Π_1				
0.5	2.57 ±0.1	1,2		
0.7	2.92 ±0.1	3		
[0ζ1] Π_2				
0.1			4.65 ±0.06	6
0.3			4.61 ±0.08	6
0.5			4.62 ±0.06	5,6
0.7			4.56 ±0.06	5
0.9			4.54 ±0.06	5
[0ζ1] Λ				
0.1	1.78 ±0.09	2		
0.2	2.27 ±0.06	2		
0.3	2.67 ±0.13	2		
0.4	3.33 ±0.07	3		
0.5			3.83 ±0.06	4
0.6			4.13 ±0.06	4
0.8			4.49 ±0.07	4

half-maximum) of the measured neutron group. In a few cases, where poor groups were obtained, the assigned errors are larger. (See note added in proof.)

IV. MODELS

The lattice vibrations of the alkali halides have been represented by three closely related formulations: the shell model used by Woods *et al.*,[4] extended by Cowley *et al.*,[16] and originally introduced by Dick and Overhauser[22]; Hardy's deformation dipole model,[14] and Tolpygo and Zaslavskaya's dipole model.[12] All the models are in the framework of the adiabatic and harmonic approximations. The Coulomb interactions and the short-range repulsive "overlap" forces are taken into account, and an attempt is made to account for the effect of the polarization of the ions on the lattice vibrations. The differences between the formulations have been discussed by Cowley *et al.*[16] We have fitted our data with the shell model, and compared the results with those due to Kucher[13] and to Tolpygo and Zaslavskaya, with Schröder's breathing-shell model,[15] and with Hardy's calculations.

The general shell model has a very large number of adjustable parameters. We have used the approximations due to Cowley *et al.* to reduce it to 11. These approximations assume that the overlap forces act only through the outer shells of valence electrons and that they extend only out to second-nearest neighbors. With axially symmetric forces, the parameters for the most general model under these assumptions are the radial and tangential short-range force constants A, B, A_{11}, B_{11}, A_{22}, and B_{22} between the K^+-Cl^-, K^+-K^+, and Cl^--Cl^- nearest-neighbor ions, respectively, the ionic charge Ze, and the electrical and mechanical polarizabilities α_1, α_2, d_1, and d_2 for the K^+ and Cl^- ions, respectively. The parameter B may be eliminated, since it is related to B_{11}, B_{12}, and Z by the stability condition $B+2B_{11}+2B_{22}=-\frac{2}{3}\alpha_M Z^2$, where $\alpha_M=1.74756$ is the Madelung constant. Noncentral forces are taken into account by introducing a parameter B'', so that B is replaced everywhere in the equations of motion by $B+B''$. The 11 independent parameters are therefore A, B'', A_{11}, B_{11}, A_{22}, B_{22}, Z, α_1, d_1, α_2, and d_2.

A modification of the model is Schröder's breathing-shell model, in which a new coordinate is introduced to express the compression (monopole) deformation of the shells. It is assumed that the spring constants between the cores and shells of the ions are the same for the compression as for the dipole deformations. This avoids the need for any new parameters.

We obtained the best-fitting values of the shell-model parameters by means of a nonlinear least-squares fit to the frequencies along certain symmetry directions using the program by Marquardt.[23] The calculation was performed on the CDC 6400 computer at the McMaster computing center. The parameters of the fits are given in Table II and the calculated frequencies are presented

[22] B. G. Dick and A. W. Overhauser, Phys. Rev. **112**, 90 (1958).

[23] D. W. Marquardt, J. Soc. Indust. Appl. Math. **11**, 431 (1963). This program is available from Share General Program Library, Catalog No. SDA 3094 (unpublished).

TABLE II. Shell-model parameters for KCl at 115°K. Parameters for model III were estimated from the bulk properties of KCl (Table IV). The parameters for all other models were obtained from the results of least-squares fitting to neutron scattering data. Parameters A_{11} and B_{11} are zero for all these models. The short-range force constants are in units of $e^2/2v$, where v is the volume of the primitive unit cell.

Model parameters	Units	I	II	III	IV	V	VI
A	$e^2/2v$	9.91 ±0.19	11.48 ±0.36	12.58	12.24 ±0.80	12.07 ±0.16	12.12 ±0.53
B	$e^2/2v$	−1.53	−1.21	0.2782	−1.08	−0.96	−1.17
B''	$e^2/2v$	0.402±0.13	0.158±0.075	−0.5884	0.02 ±0.12	···	0.075±0.07
A_{22}	$e^2/2v$	−0.14 ±0.18	−0.095±0.12	0.7587	0.01 ±0.14	···	−0.10 ±0.20
B_{22}	$e^2/2v$	0.25 ±0.084	0.060±0.050	−0.3169	0.028±0.061	···	0.058±0.047
Z	e	0.735±0.015	0.895±0.029	0.900	0.928±0.057	0.910±0.014	0.918±0.049
α_1	$1/v$	···	···	0.01974	0.034±0.014	0.028±0.006	0.028±0.010
d_1	e	···	···	0.0753	−0.060±0.071	−0.014±0.024	−0.025±0.045
α_2	$1/v$	···	0.047±0.005	0.04888	0.036±0.016	0.035±0.007	0.035±0.010
d_2	e	···	0.123±0.028	0.1865	0.087±0.086	0.131±0.022	0.121±0.028
Std. error	10^{12} cps	0.126	0.077	0.141	0.071	0.065	0.065
χ^2		9.47	2.36	4.93	2.29	1.45	1.35

in Fig. 1 as the solid line for the model that best fits the data (model VI).

The standard errors given in Table II were calculated from

$$\text{S.E.}=\left(\sum_{i=1}^{N}\frac{(\nu_{\text{obs}}{}^i-\nu_{\text{model}}{}^i)^2}{N-K}\right)^{1/2},$$

where N is the number of observations, K is the number of adjustable parameters, and the ν's are the phonon frequencies. The standard error represents an over-all average error in the fitted frequencies. We have also calculated the quantity

$$\chi^2=\frac{1}{N-K}\sum_{i=1}^{N}\left(\frac{\nu_{\text{obs}}{}^i-\nu_{\text{model}}{}^i}{\sigma_i}\right)^2,$$

where σ_i is the estimated experimental error for the ith phonon.

Table III gives some elastic and optical quantities calculated from the models and compares these with direct experiments. Table IV contains constants used in the calculations.

TABLE III. Calculated elastic constants, high-frequency dielectric constant, and small **q**-value optical frequencies for the various models of KCl. Values for the breathing-shell model, model III, are input parameters interpolated from experimental data to 115°K; ν_{LO} has been calculated using the LST relation.[a] The elastic constants are in units of 10^{11} dyn/cm^2 and the frequencies are in units of 10^{12} cps.

Model	I	II	III	IV	V	VI	Observed
C_{11}	3.15	4.46	4.60	3.53	4.76	4.72	4.60
C_{12}	0.095	0.53	0.58	0.71	0.70	0.63	0.58
C_{44}	0.583	0.73	0.653	0.73	0.70	0.72	0.653
ϵ_∞	1.0	1.73	2.15	2.22	2.08	2.08	2.15
ν_{TO}	4.39	4.42	4.36	4.41	4.43	4.41	4.36
ν_{LO}	6.36	6.35	6.36	6.39	6.33	6.34	···

[a] Reference 38.

Model I is a rigid-ion model with second-neighbor interactions between chlorine ions. The frequencies of the model are in error by up to 9%, especially along the [0ζζ] direction. The elastic constants determined from the model are in wide disagreement with the ultrasonic values.

Model II has polarizable chlorine ions. The standard error has been reduced considerably, and the elastic constants obtained are closer to the experimental values than those of model I. The high-frequency dielectric constant is still in considerable error.

Model III is the breathing-shell model and was not fitted to the neutron-scattering data. Its parameters were estimated from the values of the bulk properties of KCl interpolated to 115°K, given in Table III. Dispersion curves for this model are plotted for comparison with the data as the dashed curve in Fig. 1. The over-all agreement with experiment of the calculated dispersion curves is quite good. The value of ν_{LO} at small **q** values is in excellent agreement, but there are discrepancies in the initial slopes of the longitudinal branches and the agreement around point X is not very good. The parameters of model III were used as the initial guess in all the least-squares fits.

Model IV is a fitted breathing-shell model. The fit is slightly improved over model II, and the high-frequency dielectric constant is in good agreement with experiment. However, the elastic constants now show discrepancies.

Note that the change in going from a breathing-shell model fitted to macroscopic parameters to one fitted to neutron measurements is not large, particularly in the case of the short- and long-range polarizabilities. This implies that within the breathing-shell-model framework the neutron measurements are in agreement with the macroscopic constants.

Model V is a six-parameter shell model with both ions polarizable and no second-neighbor repulsive forces. Model VI includes second-neighbor repulsive forces

between chlorine ions and has a parameter to allow for noncentral forces. The errors of these last two models are essentially the same. Model VI gives a slightly better fit than model V to ν_{TO} at small $\mathbf{q}$. The mechanical polarizability of the K^+ ion in models IV–VI, while negative, is smaller than the error associated with it, so that no significance should be attached to its sign.

Another model with the full 11 parameters adjustable gave no significant improvement in fit and is not included in Table II. Model VI was therefore selected as the best model for the purpose of reproducing the frequencies and was used in all the subsequent calculations.

Figure 1 also shows Kucher's[13] calculated values as the dotted curve. The agreement with the neutron measurements is generally good. Similarly the calculations of Hardy are in qualitative agreement with experiment, although discrepancies of the order of 10% are common in both cases. Some of these variations might be due to the use of room-temperature macroscopic constants in the fitting. It can be seen, however, that even when parameters interpolated to 115°K (model III) are used, the standard error is more than twice as large as for model VI, fitted directly to neutron data.

V. CALCULATIONS FROM MODEL VI

A. Frequency Distributions

The frequency distribution function $g(\nu)d\nu$ is shown in Fig. 2. It was obtained by solving the shell-model dynamical matrix in the octant $0<q_x<2\pi/a$, $0<q_y<2\pi/a$, and $0<q_z<2\pi/a$ at 10 000 randomly chosen points. The frequencies were sorted into a histogram containing 127 bins. Figure 3 shows the frequency spectrum ordered according to the branch index j: at each $\mathbf{q}$, the six frequencies are numbered $j=1, \cdots, 6$ in order of increasing size. Figure 3 also shows the location of some of the symmetry points as given by model VI. For the phonons at Γ and X, the model differs from experiment by less than 2%. The whole $[\zeta\zeta\zeta]$ TA branch, however, is predicted high by the model and the zone-boundary frequency could be as much as 7 cm^{-1} lower than the value predicted by the model (106.2 cm^{-1}).

TABLE IV. Values of constants used in the KCl calculations.

$\frac{1}{2}a=r_0=3.12$ Å	$\nu_{TO}=4.36\times10^{12}$ cps[a]
$v=2r_0^3=60.8$ Å^3	$\alpha_1=1.201$ Å^3 [b]
$e^2/2v=1896$ dyn/cm^2	$\alpha_2=2.974$ Å^3 [b]
$M_+=39.102$ amu	$C_{11}=4.60\times10^{11}$ dyn/cm^2 [c]
$M_-=35.457$ amu	$C_{12}=0.58\times10^{11}$ dyn/cm^2 [c]
$\epsilon_\infty=2.15$[b]	$C_{44}=0.653\times10^{11}$ dyn/cm^2 [c]
$\epsilon_0=4.57$[e]	

[a] See the Appendix.
[b] J. R. Tessman, A. H. Kahn, and W. Shockley, Phys. Rev. **92**, 890 (1953).
[c] Interpolated to 115°K from M. H. Norwood and C. V. Briscoe, Phys. Rev. **112**, 45 (1958).
[d] Interpolated to 115°K from M. Born and K. Huang, *Dynamical Theory of Crystal Lattices* (Oxford University Press, Oxford, 1954), Table 17, p. 85; and from D. H. Martin, Advan. Phys. **159**, 223 (1960).
[e] Interpolated to 115°K from M. C. Robinson and A. C. H. Hallett, Can. J. Phys. **44**, 2211 (1966).

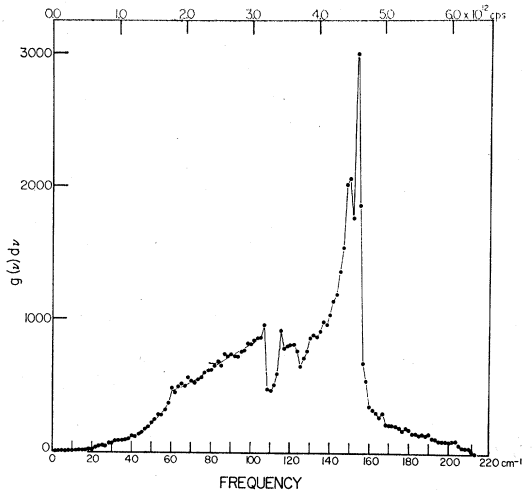

FIG. 2. Total frequency distribution calculated from model VI using 10 000 randomly selected wave vectors sorted into 127 bins.

It can be seen that the zone-boundary symmetry points do not, in general, correspond to very distinct features in the total $g(\nu)$ curve. It has been customary to use points X and L to explain peaks in the second-order Raman spectra.[24] With the exception of the lowest X frequency there seems to be little justification for this procedure at present.

The very strong peak at 155 cm^{-1} arises from a saddle-point in the sixth branch, which does not correspond to any of the symmetry points. This peak has been seen by

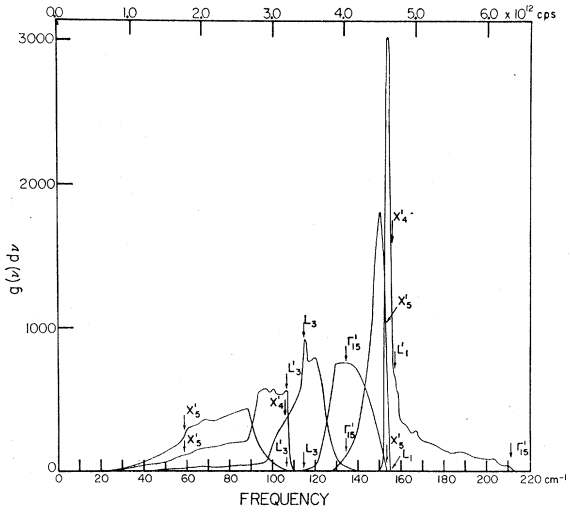

FIG. 3. Individual frequency distributions for the six branches, for the 10 000 wave vectors of Fig. 2. The points have been omitted for clarity. The frequencies of the symmetry points Γ, X, and L are shown for each branch.

[24] E. Burstein, F. A. Johnson, and R. Loudon, Phys. Rev. **139**, 1239 (1965).

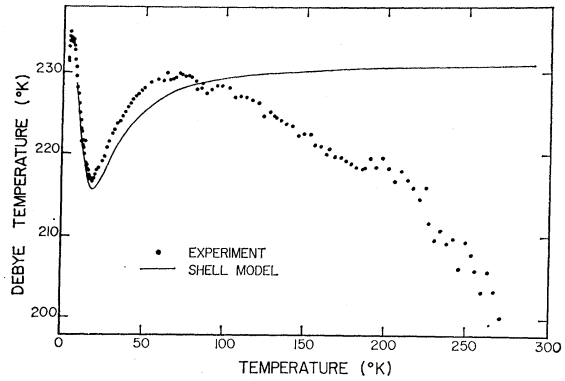

FIG. 4. Debye characteristic temperature Θ_D obtained from the heat capacity. The theoretical curve was calculated from model VI. The experimental points were derived from C_p measurements (Ref. 29), which were first corrected to give C_v.

Callender and Pershan[25] in the second-order helium-temperature Raman spectrum of KCl at 2×155 cm^{-1} and in the fluorescence sideband of KCl:Sm^{++} by Bron.[26] The half-width of this peak in the samarium fluorescence is only 2.5 cm^{-1} and its position is 156 cm^{-1}.[27]

The peak at 107 cm^{-1} is related to a near-degeneracy of a saddlepoint at (0.51, 0.51, 0) and a maximum near (0.5,0.5,0.5). This singularity is of some interest since it occurs in all alkali-halide crystals for Σ_4 symmetry branches at this point in the zone. Measurements of the impurity-induced far-infrared absorption in KBr show that the rise in the second branch from the saddle point to the maximum occurs in a 0.3-cm^{-1} interval. A similar effect should be observable in KCl near 107 cm^{-1}.

B. Heat Capacity, Debye Temperature, and Debye-Waller Factor

Using Eqs. (14.1) and (2.3) of Blackman,[28] the heat capacity C_v and Debye temperature Θ_D have been calculated from the frequency distribution function $g(\nu)$. The calculation is compared with the experimental measurements of Berg and Morrison[29] in Fig. 4. At very low temperatures Θ_D is sensitive to the low-frequency part of $g(\nu)$; the calculated values depend on the method of calculating $g(\nu)$ and have been omitted from the figure. Using de Launay's[30] procedure, and the elastic constants predicted by model VI, we obtain $\Theta_D(0)=241$°K. Estimating the initial slopes of the dispersion curves (and hence the elastic constants) gives $\Theta_D=238$°K.

In the low-temperature region, the calculated curve lies a few degrees below the experimental points. Better agreement would be expected if a frequency distribution appropriate to the temperature T were used to obtain $\Theta_D(T)$. At high temperatures, the experimental values fall off rapidly. This is interpreted as an anharmonic effect, since the harmonic approximation predicts that Θ_D becomes constant at high temperatures.

For a cubic crystal, the Debye-Waller factor W_i is related to the total mean-square displacement $\langle u_i^2\rangle$ of ion i by

$$2W_i=\tfrac{1}{3}Q^2\langle u_i^2\rangle,$$

where[31]

$$\langle u_i^2\rangle=\frac{h}{4\pi^2NM_i}\sum_{\mathbf{q}j}\frac{|\mathbf{e}_{ij}(\mathbf{q})|^2}{\nu_j(\mathbf{q})}[n_j(\mathbf{q})+\tfrac{1}{2}].$$

Here $\mathbf{e}_{ij}(\mathbf{q})$ is the eigenvector of the ith ion in the $(\mathbf{q},j)$ normal mode and $n_j(\mathbf{q})=(e^{h\nu_j(\mathbf{q})/k_BT}-1)^{-1}$.

The quantity $B_i=\tfrac{1}{3}8\pi^2\langle u_i^2\rangle$ has been calculated using individual frequency distribution functions[1] for the two ions, and is shown in Fig. 5.

The experimental measurements[32,33] of B_i are in poor agreement with the calculation. The experimental difficulties have been pointed out by Buyers and Smith,[34] and in view of this the disagreement is not surprising.

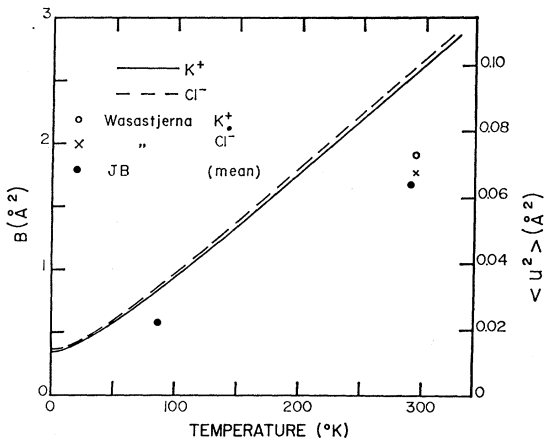

FIG. 5. Debye-Waller parameter B and the total mean-square displacement $\langle u^2\rangle$ for the K^+ and Cl^- ions. The curves were calculated from model VI. The points are the measurements of Wasastjerna (Ref. 33) and of James and Brindley (JB, Ref. 32).

[25] R. H. Callender and P. S. Pershan, in Proceedings of International Conference on Light Scattering Spectra of Solids, New York University, 1968 (unpublished).

[26] W. E. Bron, Phys. Rev. **140**, A2005 (1965).

[27] M. Buchanan (private communication).

[28] M. Blackman, in *Handbuch der Physik*, edited by S. Flügge (Springer-Verlag, Berlin, 1955), Vol. VII, Pt. 1.

[29] W. T. Berg and J. A. Morrison, Proc. Roy. Soc. (London) **A242**, 467 (1967).

[30] J. de Launay, J. Chem. Phys. **30**, 91 (1959).

[31] A. A. Maradudin, E. W. Montroll, and G. H. Weiss, *Theory of Lattice Dynamics in the Harmonic Approximation* (Academic Press Inc., New York, 1963).

[32] R. W. James and G. W. Brindley, Proc. Roy. Soc. (London) **A121**, 162 (1928).

[33] J. A. Wasastjerna, Soc. Sci. Fennica Commentationes Phy. Math., **13**, 1 (1946); quoted in *International Tables for X-Ray Crystallography*, edited by K. Lonsdale (Kynoch Press, Birmingham, England, 1962), Vol. III, p. 240.

[34] W. J. L. Buyers and T. Smith, J. Phys. Chem. Solids **25**, 483 (1964).

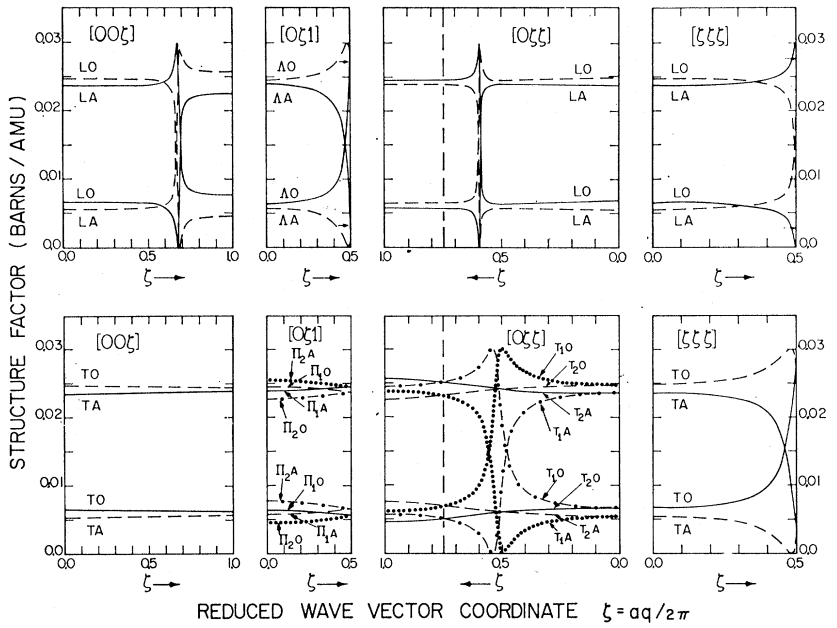

FIG. 6. Reduced inelastic structure factor $|f|^2$ for the major symmetry directions in KCl, calculated from model VI. The labelling of the branches is as in Fig. 1. The solid and dot-dash lines are calculated for a reciprocal-lattice vector τ having even indices. The dashed and dotted lines are for τ with odd indices. The arrows in the upper diagrams indicate the value of $|f|^2$ at $(0,\frac{1}{2},1)$ and $(\frac{1}{2},\frac{1}{2},\frac{1}{2})$.

C. Inelastic Structure Factor

The intensity of a (one-phonon) neutron group $(\mathbf{q},j)$ observed in a constant-$\mathbf{Q}$ scan is[35,36]

$$I=N\left(\frac{k'}{k_0}\right)\frac{\hbar[n_j(\mathbf{q})+\frac{1}{2}\pm\frac{1}{2}]}{4\pi\nu_j(\mathbf{q})}|F|^2,$$

where N is the number of primitive cells in the crystal, and the upper (lower) sign refers to phonon creation (annihilation). The structure factor $|F|^2$ is given by

$$|F|^2=|\sum_i b_i e^{i2\pi\tau\cdot\mathbf{r}_i}\mathbf{Q}\cdot\mathbf{e}_{ij}(\mathbf{q})M_i^{-1/2}e^{-W_i(\mathbf{Q})}|^2,$$

where b_i, $\mathbf{r}_i$, M_i, and W_i are the coherent scattering length, position vector, mass, and Debye-Waller factor, respectively, for the ith atom or ion. For wave vectors along a symmetry direction in KCl, this reduces to

$$|F|^2=(\mathbf{Q}\cdot\hat{V})^2|b_1M_1^{-1/2}e^{-W_1(\mathbf{Q})}\xi_{1j}(\mathbf{q}) \pm b_2M_2^{-1/2}e^{-W_2(\mathbf{Q})}\xi_{2j}(\mathbf{q})|^2,$$

where $\hat{V}$ is a unit vector in the direction of the polarization vector of ion 1, and $\hat{V}\xi_i=\mathbf{e}_i$: The upper (lower) sign is used when the reciprocal-lattice vector τ involved [see Eq. (2)] has even (odd) indices; subscripts 1 and 2 refer to the K^+ and Cl^- ions, respectively.

The Debye-Waller factors W_i, for $\mathbf{Q}=(0,0,6)\times 2\pi/a$ and $T=100°$K, are $W_1=0.211$, $W_2=0.216$, and $e^{-W_1}/e^{-W_2}=1.005$. We may therefore neglect the difference in the Debye-Waller factors and write

$$|F|^2=(\mathbf{Q}\cdot\hat{V})^2e^{-2W_{\rm av}(\mathbf{Q})}|f|^2,$$

where the "reduced inelastic structure factor"

$$|f|^2=|b_1M_1^{-1/2}\xi_{1j}(\mathbf{q})\pm b_2M_2^{-1/2}\xi_{2j}(\mathbf{q})|^2.$$

Using the values[20] $b_1=0.34_5$ and $b_2=0.98$, and eigenvectors calculated from model VI, $|f|^2$ has been calculated for the major symmetry directions and is shown in Fig. 6. The curves show important differences from the analogous curves for NaI [4] and LiF,[1] principally because of the similarity of the ionic masses and because of the large ratio of the scattering lengths.

Comparison with the dispersion curves (Fig. 1) indicates that rapid changes in $|f|^2$ occur whenever the separation of the acoustic and optic branches of the same polarization has a minimum value. At such points the two acoustic curves (for even and odd τ) intersect, indicating that one of the ions is stationary. Similarly the two optic curves cross, and for this mode the other ion is stationary. For phonons $(\mathbf{q},j)$ at (0,0,0.68) LA, (0,0.5,1) ΛO, (0,0.6,0.6) LO, (0.5,0.5,0.5) LA and TO, and (0,0.51,0.51) T_1O, only the Cl^- ions are moving and $|f|^2=b_{Cl}^2/M_{Cl}\simeq 0.027$ b/amu. At (0,0,0.68) LO, (0,0.5,1) ΛA, etc., the Cl^- ions are stationary and $|f|^2=b_K^2/M_K\simeq 0.003$. For all values of τ the former modes are about nine times as intense as the latter modes and only the former modes can be observed. This effect is fortunately limited to very small regions in $\mathbf{q}$, particularly in the longitudinal cases.

VI. CONCLUSION

We have presented measurements of phonon frequencies along the major symmetry directions in KCl at 115°K. Neutron groups of well-defined frequency and polarization were observed at all $\mathbf{q}$ values except near $(\frac{1}{2},\frac{1}{2},\frac{1}{2})\times 2\pi/a$. The frequencies found agreed quite well

[35] I. Waller and P. O. Froman, Arkiv Fysik 4, 183 (1952).
[36] B. N. Brockhouse and P. K. Iyengar, Phys. Rev. 111, 747 (1958).

with a shell-model calculation based on macroscopic parameters; if the parameters are allowed to vary to give a best fit to the neutron measurements the agreement is further improved. The polarizabilities that are obtained in this way do not take on unphysically large negative values as was observed in KBr.

In the case of KCl at least, it seems that the shell model, in its various forms, offers a good description of the dynamical behavior of the lattice. KCl seems to behave very much like an ideal ionic crystal; even the rigid-ion model gives a fit that has only twice the standard error of the best shell model.

Using the best least-squares-fit shell model we have calculated some properties of KCl. The frequency distribution $g(\nu)$ shows the characteristic sharp peaks associated with saddle points in the frequency spectrum, the strongest of which can also be found in the Raman spectrum of KCl. Up to about 70°K the Debye temperature calculated from $g(\nu)$ is in good agreement with data from specific heats.

One of the main motivations for undertaking this work has been to provide good phonon frequencies for use in interpreting other experiments, in particular those optical effects where phonons play an important role.

Note added in proof. Recently G. Raunio and L. Almqvist have measured dispersion curves in KCl at 80 and 300°K, by neutron inelastic scattering. Their results are generally in good agreement with our own. Their measurements of the $[\zeta\zeta\zeta]$ TA branch, however, lie as much as 7% higher. Since the higher frequencies are in better agreement with our model VI (see Sec. IV), and since these workers took extra care to investigate the dispersion surfaces in the vicinity of this branch, we believe their results for this branch are more reliable than our own.

ACKNOWLEDGMENTS

We are grateful to Professor B. N. Brockhouse for his assistance and encouragement. Our thanks to our colleagues at McMaster for helpful discussions, in particular E. R. Cowley and M. Buchanan, and G. A. deWit (now at Rutgers University, New Brunswick, N. J.) for his assistance with some of the measurements. J. A. Morrison kindly sent his complete heat-capacity results and U. Schröder assisted us with the breathing-shell-model calculations. We are grateful to Atomic Energy of Canada, Ltd., for their support.

APPENDIX: TO FREQUENCY AT $q \rightarrow 0$

At the time of these measurements we were unable to find in the literature a recent measurement of the transverse ($\mathbf{q} \rightarrow 0$) optical frequency. We made a determination of $\nu_{TO}(\mathbf{q} \rightarrow 0)$ ourselves with a far-infrared spectrometer on evaporated thin films of KCl. Such measurements are very difficult to interpret because of the importance of surface effects resulting from the very small penetration of the light. The observed peaks are generally very much broader than one would expect[37] for optical phonons. We also found an effect due to the differential expansion of the substrate which we attempted to correct for by extrapolating from quartz and lithium-fluoride substrates to a hypothetical KCl substrate. Our results are summarized in Table V, and

TABLE V. Lyddane-Sachs-Teller relation[a] and comparison with infrared absorption (reststrahlen) frequency.

T (°K)	$\nu_{LO}(\mathbf{q} \rightarrow 0)$ Neutrons (10^{12} cps)	$\nu_{TO}(\mathbf{q} \rightarrow 0)$ Neutrons (10^{12} cps)	$\nu_{TO}(\mathbf{q} \rightarrow 0)$ Infrared (10^{12} cps)	$(\epsilon_0/\epsilon_\infty)^{1/2}$	$(\nu_{LO}/\nu_{TO})_{\mathbf{q}\rightarrow 0}$ Neutrons
4.2			4.50±0.03		
115	6.39±0.1	4.39±0.03	4.36±0.07	1.46	1.46
300		4.19±0.05	4.19±0.07		

[a] Reference 38.

it can be seen that they agree with the neutron measurements. Table V also gives a comparison of our measured frequencies at $\mathbf{q} \rightarrow 0$ with the prediction by Lyddane, Sachs, and Teller[38] (the LST relation). It will be seen that this relation, $\omega_{LO} = (\epsilon_0/\epsilon_\infty)^{1/2}\omega_{TO}$, holds for KCl. This is in agreement with results for the other alkali halides.

[37] E. R. Cowley and R. A. Cowley, Proc. Roy. Soc. (London) **A287**, 259 (1965).

[38] R. H. Lyddane, R. G. Sachs, and E. Teller, Phys. Rev. **59**, 73 (1941).